MR1 dependent MAIT cell activation is regulated by autophagy associated proteins

Prabhjeet Phalora[1], James Ussher[1,3], Svenja Hester[2], Emanuele Marchi[1], Jeffrey Y. W. Mak[4], David P. Fairlie[4], Paul Klenerman[1*]

[1]Peter Medawar Building for Pathogen Research, University of Oxford, Oxford, OX1 3SY, UK

[2]Advanced Proteomics Facility, Department of Biochemistry, University of Oxford, Oxford, OX1 3QU, UK

[3]Department of Microbiology and Immunology, University of Otago, 720 Cumberland Street, Dunedin 9054, New Zealand

[4]Institute for Molecular Bioscience, The University of Queensland, Brisbane, Queensland 4072, Australia

[*]Correspondence: paul.klenerman@medawar.ox.ac.uk

Abstract

The antigen presenting molecule, MR1, presents microbial metabolites to MAIT cells, a population of innate-like, anti-microbial T cells. It also presents an unidentified ligand to MR-1 restricted T cells in the setting of cancer. The cellular co-factors that mediate MR1 antigen presentation have yet to be fully defined. We performed a mass spectrometry-based proteomics screen to identify MR1 interacting proteins and identified the selective autophagy receptor SQSTM1/p62. CRISPR-Cas9-mediated knock out of SQSTM1/p62 increased MAIT cell activation in the presence of *E.coli* but not the synthetic ligand 5-OP-RU whereas depletion of Atg5 and Atg7, key autophagy proteins, increased MAIT activation irrespective of the ligand used. This regulation appears to occur at an early step in the trafficking pathway. This data implicates distinct roles for autophagy associated proteins in the regulation of MR1 activity and highlights the autophagy pathway as a key regulator of cellular antigen presentation.

Keywords

MR1, MAIT cells, antigen presentation, autophagy, SQSTM1, Atg5, Atg7

Introduction

Major Histocompatibility Related Protein 1 (MR1) is an evolutionary conserved, monomorphic, MHC like protein that presents microbial metabolites derived from vitamin B2 biosynthesis to a population of anti-bacterial innate-like CD8+ or double negative T cells termed Mucosal Associated Invariant T (MAIT) cells [1]. MAIT cells express high levels of CD161 and the semi invariant TCR Vα7.2 and, upon activation, produce inflammatory cytokines such as IL17 and IFNγ as well as the cytolytic granules TNFα and Granzyme B [2–4] The microbial ligands that bind to MR1 and activate MAIT cell effector functions are unstable pyrimidine intermediates, including 5-(2-oxoethylideneamino)-6-D-ribitylaminouracil (5-OE-RU) and pyrimidine-5-(2-oxopropylideneamino-6-D-ribitylaminouracil (5-OP-RU) formed by the condensation of the riboflavin biosynthetic precursor 5-amino-6-D-ribitylaminouracil (5-A-RU)) with glyoxal and methylglyoxal, respectively [5–7] In general, only microbes that generate riboflavin can activate MAIT cells [8]. However, the identification of MR1T cells, a novel population of T cells with diverse TCRs that are restricted by MR1 in the absence of bacteria, suggest that MR1 also presents non-microbial, endogenously derived ligands, including cancer specific antigens [9–12]. The recognition of as yet unidentified self-antigen(s) by MR1, as well as its non-polymorphic nature, make it an ideal candidate for the development of cancer immunotherapies and highlights the need for a better understanding of MR1 biology.

MR1 is expressed in most, but not all, mammalian species with a high degree of sequence conservation, particularly in the ligand binding domains [13]. Although MR1 mRNA is expressed in a variety of tissues and cell types, cellular protein levels and distribution appear to be tightly regulated and MR1 is difficult to detect at the cell surface, even after antigen exposure [14–16]. This is in contrast to other MHC molecules which are constitutively expressed and readily detectable at the plasma membrane (PM). The mechanisms that govern this regulation remain poorly defined, although innate signalling molecules appear to be important [17,18]. Previous studies, mainly using over-expressed protein, have reported that the majority of MR1 is localized to the endoplasmic reticulum (ER) [19–22], but it can also be found in the trans-Golgi network, endosomes and lysosomes [13,14,23]. ER resident MR1 is believed to be unbound and in an unfolded conformation. Upon interaction with its ligand, which forms a covalent bond with the sidechain of lysine 43, MR1 undergoes a conformational change that facilitates binding to β2M. This ternary complex exits the ER and traffics to the PM [19,24]. Surface MR1 is rapidly degraded or recycled through endosomes. Little to no MR1 can be detected on the cell surface in the absence of antigen, which indicates that on the whole only ligand bound, fully folded MR1 can leave the ER. However, in some instances conformational changes leading to surface expression can occur in the absence of known ligands [17,25].

Due to the inherently low expression of MR1, it has been difficult to resolve the cellular proteins, apart from β2M, that are involved in its trafficking from the ER to the PM to facilitate T cell activation [20–22].

Several groups have reported interactions between MR1 and components of the peptide loading complex (PLC), more commonly associated with MHC Class I trafficking [14]. This is supported by recent work from McWilliams et al, who demonstrated a key role for TPN and TAPBR in maintaining a pool of unbound MR1 in the ER, preventing its degradation before antigen exposure [26]. Additionally, loss of the ER associated P5-ATPase ATP13A1, a putative membrane transporter, reduced MR1 intracellular and surface protein levels [27]. Once MR1 has exited the ER, certain Rab and SNARE proteins may be important for trafficking to the Golgi, as reported in the context of *M. tuberculosis* infection [23]. Whether these findings are applicable in response to other microbes or sources of antigen remains to be determined.

Thus, the molecular machinery that governs MR1 cell surface expression and function has yet to be fully determined, and other unexplored pathways could be important. For instance, it was reported that MHC Class I internalization was regulated by autophagy [28]. Specifically, the removal of key autophagy proteins *in vivo* resulted in increased Class I expression at the PM, due to impaired receptor-mediated endocytosis and hence greater CD8+ T cell responses to viral infection. Autophagy is a key intracellular quality control pathway for the removal of damaged and defective cellular components. It is elevated in response to stress, which leads to the activation of mTOR kinase and formation of the autophagosome [29–31]. This double membrane structure elongates and matures to engulf the targeted material, which is then degraded upon fusion with a lysosome [32]. Each step of this process is carefully controlled by members of the Atg protein family [33]. Whether autophagy also contributes to regulation of MR1 cell surface expression and hence antigen presentation is unknown.

We aimed to identify the network of cellular proteins that interact with MR1 in bacterially exposed cells, by utilizing immunoprecipitation combined with mass spectrometry to perform a global, unbiased proteomics screen. Many of the proteins identified have known roles in antigen presentation, but several others, including components of the autophagy pathway, were also discovered. Thus we sought to explore the role of autophagy and associated proteins in the regulation of MR1 expression and activity.

Results

A proteomics screen to define MR1 associated proteins during antigen presentation

Proteins that interact with MR1 may play an important role in its regulation as well as its function in antigen presentation. In order to identify these proteins, we used a Thp1 cell line stably expressing a HA tagged MR1 construct (Thp1.MR1.HA). Thp1 cells are a monocytic antigen-presenting cell (APC) line that express low levels of endogenous MR1 and can efficiently activate MAIT cells in a co-culture experiment. The tagged MR1 construct has been shown to be fully functional akin to the wild-type protein [17]. Thp1 and Thp1.MR1.HA cells were incubated overnight with fixed *E. coli* and MR1 was immunoprecipitated using an antibody directed against the HA tag. Eluted samples were analyzed by liquid chromatography tandem mass spectrometry (LC-MS/MS) to identify cellular proteins that

specifically associate with MR1 in the presence of antigen. As expected, β2M, a protein necessary for MR1 function, was identified as a significant MR1-interacting protein by this method, confirming the validity of this approach (Figure 1A and Supplementary Table S1). Several other proteins with known roles in antigen presentation and associated with the ER were also recovered, including Tap, Tapasin (TAPBP), Calnexin (CANX) and Calreticulin (CALR) (Figure 1A and 1B). In addition, proteins not previously reported to interact with MR1 were also identified, several of which have functions linked to ER degradation (SEL1L, AUP1, EDEM1) and autophagy (SQSTM1/p62, TMEM173/STING, TMEM59, LAMP-3) in particular. Interestingly, the alpha subunit of IL23 was identified as one of the proteins most highly associated with MR1. IL23 modulates the inflammatory response to infections via activation of the JAK-STAT pathway and contributes to several inflammatory and autoimmune diseases [34–36] Overall, these data confirm earlier studies linking MR1 with proteins associated with antigen processing and presentation, particularly the PLC. However, they also demonstrate that the cellular network of MR1 interacting proteins may be more expansive than previously described.

Ligand dependent cytokine induction may alter the composition of the MR1 proteome

Next, we sought to validate the interactions between MR1 and several of the proteins identified by the proteomics screen. Immunoprecipitated MR1.HA, from Thp1.MR1.HA cells incubated with fixed *E. coli* overnight was run on SDS-PAGE gels and then probed with specific antibodies targeting the proteins of interest. β2M was efficiently co-immunoprecipitated with MR1 by this method. Components of the PLC, including Calnexin, Tapasin and Calreticulin were found to associate with MR1 (Figure 1C). SEL1L and SQSTM1, which were identified by the mass spectrometry analysis, were also pulled down in the presence of MR1 but IL23A and TMEM173/STING were not (Figure 1C and Supplementary Figure 1). When the co-immunoprecipitations were performed in the presence of the synthetic MR1-binding ligand 5-OP-RU, rather than *E. coli*, these interactions could no longer be recapitulated, except for β2M and more weakly Calnexin (Figure 1D). Reducing the incubation period from overnight to 2 hours still did not recover all of the interactions as observed with *E.coli* (Supplementary Figure 1B). These results suggest that other components of *E.coli* may be affecting engagement with cellular proteins as has been previously reported [11,16,37]. This may be supported by the observation that co-incubation of Thp1.MR1.HA cells with fixed *E. coli* leads to an increase in MR1.HA (and to a lesser extent SQSTM1) protein expression, even at lower bacteria to cell ratios (Supplementary Figure 1C), possibly due to changes in the cellular cytokine environment that promotes MR1 expression and/or stabilization. This was not observed when the cells were treated with synthetic 5-OP-RU alone. Interestingly, 5-OP-RU was able to affect MR1 protein levels in the presence of the cytokines IL12 and IL18, which likely more closely reflects the cellular conditions induced by *E. coli* (Supplementary Figure 1D). However, incubation with 5-OP-RU and IL12/18 still did not result in a detectable interaction between MR1 and SQSTM1 (Supplementary Figure 1E). Further, use of IL12 and IL18 blocking antibodies did not prevent an increase in MR1 expression when the cells were also incubated with *E.coli* (Supp Figure 1F), indicating that other cytokines/bacterial interactions must also be important. Thus the composition of the

MR1 proteome may differ according to the presence and nature of the ligand involved and may also be modulated by cytokine responses.

Knock-out of the autophagy adaptor protein SQSTM1 leads to increased MAIT cell activation in the presence of E.coli

We focused on the autophagy associated protein SQSTM1 (also known as p62) because in the presence of *E.coli* its expression levels increased and it consistently interacted with MR1 in our system. SQSTM1 is an adaptor molecule that binds to ubiquitinated cargo in the ER through its UBA domain and LC3 through its LIR domain, to target proteins to autophagosomes for degradation via selective autophagy [38,39]. It also has roles in several cellular signalling pathways [40,41]. In order to understand the functional significance of the MR1-SQSTM1 interaction, we utilized CRISPR-Cas9 technology to knock out SQSTM1 (and β2M as a positive control) from wild-type Thp1 cells (expressing endogenous levels of MR1) and established single-cell clones by limiting dilution. All clones were verified by immunoblot analysis and sequencing (Figure 2A). These cells were then incubated with either DMSO, fixed *E. coli* 5-OP-RU or the non-MAIT stimulatory synthetic ligand Ac-6-FP overnight and levels of surface MR1 were compared. Both β2M knockout clones (B1 and B6), showed substantially reduced MR1 surface staining in all conditions tested, as expected (Figures 2B and 2C). However, the results from the SQSTM1 knockout clones (S1, S2, S3 and S4) were more variable (Figures 2B and 2C). There were no significant differences between the clones and the control cell line in the *E.coli* condition, however two of the clones (S1 and S4) displayed significantly reduced MR1 surface levels in the presence of 5-OP-RU and Ac-6-FP. Surface MHC Class I levels were mostly not affected in these clones (Supplementary Figure 2A).

To assess whether these changes impacted MR1 antigen presentation, we performed an assay to measure levels of MAIT cell activation. β2M and SQSTM1 knock out clones were incubated with *E. coli* or 5-OP-RU overnight and then co-cultured with purified CD8+ T cells for 5 hours. IFNγ production from the CD161++ Vα7.2+ population was measured by FACS (Figure 2D). In cells depleted of β2M there was a significant reduction in MAIT cell activation in both the *E. coli* and 5-OP-RU conditions (Figure 2D). In contrast, we observed a significant increase in IFNγ production from MAIT cells after incubation with the SQSTM1 knock out cells but interestingly only in the presence of *E. coli* and not with 5-OP-RU, where MAIT activation was either unaffected or decreased compared to the control (Figure 2D, right panel). A second set of clonal cells derived from a different guide RNA targeting SQSTM1 also showed an increase in MAIT cell activation following *E.coli* stimulation and a significant decrease with 5-OP-RU stimulation (Supplementary Figures 2B and 2C). The only exception to this was the Thp1 clone #5, which actually showed a significant decrease in the presence of *E.coli* (Supplementary Figure 2C). This clone grew substantially slower than the others, which may explain its contrasting phenotype. The increase in MAIT cell activation in the presence of *E.coli* was also observed in the bulk population of cells before generation of the clonal lines (Supplementary Figure 2D) and was blocked with the use of an anti-MR1 antibody (data not shown). These results could also be reproduced when SQSTM1-depleted

C1R cells, a B cell line, were used as the APC instead of Thp1 cells (Supplementary Figures 2E and 2F). Overall, in the absence of SQSTM1, cellular changes induced by *E.coli* result in increased antigen presentation, which is not replicated with 5-OP-RU where MAIT activation may be adversely affected, implying that regulation of MR1 function by SQSTM1 may be dependent on the nature of the antigen.

Depletion of Atg5 and Atg7 increases MAIT cell activation

The varied results observed with knockout of SQSTM1 on MAIT cell activation in the presence of fixed *E.coli* versus 5-OP-RU could be attributable to the multiple other cellular functions of this protein, distinct from autophagy. Additionally, although SQSTM1 is an important component of selective autophagy, its role may be functionally redundant with other similar adaptor proteins such as NBR1 [39,42]. In order to determine the effects of autophagy more precisely on MRI function we targeted two essential components of the autophagy machinery. Atg5 and Atg7 have significant roles in the formation of the autophagosome and are routinely depleted *in vitro* and *in vivo* to study the effects of autophagy. Reduced expression of these proteins in wild-type Thp1 cells by CRISPR –Cas9 treatment (Figure 3A) led to impaired autophagy in these cells (Supplementary Figure 3A and 3B), as assessed by the substantial reduction in levels of lipidated membrane bound LC3B (LC3B-II), a marker of fully formed autophagosomes [43]. Surface MR1 levels in Atg5 and Atg7 CRISPR-Cas9 treated cells were moderately increased after incubation with *E. coli* and 5-OP-RU compared to control cells, although these differences were not statistically significant (Figure 3B). In addition, IFNγ production by MAIT cells was also increased after co-culture with these cell lines (Figure 3C). This was also true when 5-OP-RU was used as the ligand instead of *E. coli* (Figure 3D) and when C1R cells were used as the APC rather than Thp1s (Supplementary Figure 4A-D), in contrast to the results found with knock out of SQSTM1. The use of multiple guide RNAs against two separate proteins in the autophagy pathway with similar outcomes means that it is less likely that the observed phenotypes are due to off-target effects.

As surface MR1 levels were not significantly increased in the autophagy-deficient cells, we generated Thp1.MR1.HA cells transduced with Atg5 and Atg7 gRNAs to check total protein levels by western blot. MR1 protein expression was higher in the Atg-depleted cells compared to the control cells, even at baseline (Supplementary Figure 5). The same was true for SQSTM1, a protein known to be regulated by autophagy, whereas other ER resident proteins remained unchanged. We also sought to determine whether any of the interactions we previously found with MR1 (Figure 1C) were altered in the absence of autophagy. There appeared to be no differences in protein interactions between MR1 and β2M, SQSTM1, Calnexin and Tapasin, in control versus knockdown cell lines (Supplementary Figure 5). Taken together, these results demonstrate that MR1 protein levels are upregulated in autophagy-deficient cells intracellularly and to a lesser extent at the cell surface. These changes in protein expression have a significant impact on MR1 antigen presentation and subsequently MAIT cell activation, implicating the autophagy pathway in the regulation of MR1 activity.

Manipulation of autophagy alters MR1 intracellular and surface expression levels

As a complementary approach we also used a panel of chemical reagents to manipulate the autophagy pathway. 3MA and wortmannin are PI3K inhibitors which prevent activation of mTOR and thus block autophagosome formation at an early stage [29,43]. Treatment of Thp1.MR1.HA cells with these inhibitors led to an increase in total MR1 protein levels as determined by western blot (Figure 4A). Amino acid starvation of cells induces autophagy and subsequent treatment with bafilomycin prevents the autophagosomes from fusing with lysosomes and being degraded. Incubation of Thp1.MR1.HA cells in EBSS media, which lacks amino acids, slightly increased MR1 levels but was not further enhanced with subsequent addition of bafilomycin (Figure 4A). Imaging of HeLa.MR1.HA cells also showed an increase in MR1 cytoplasmic signal intensity following treatment with the autophagy inhibitors and inducers, particularly with 3MA. SQSTM1 is mainly found in discrete cytoplasmic foci, most likely p62 bodies as has previously been described [44], which become more numerous and concentrated following EBSS +/- bafilomycin treatment.

Following on from this we specifically looked at MR1 surface levels in human primary monocytes and Thp1.MR1.HA cells. Surface MR1 levels were significantly increased in primary monocytes with the addition of bafilomycin and wortmanin and significantly decreased following EBSS treatment (Figure 4C). Similar trends were also observed in Thp1.MR1.HA cells. Pre-incubation with 5-OP-RU before addition of the autophagy inhibitors further elevated MR1 surface expression significantly compared to the control condition in both cell types. Surprisingly, this increase was also seen when autophagy was enhanced with the use of EBSS (Figure 4B, right graphs), indicating that the addition of antigen can rescue MR1 bound for degradation via autophagy. Therefore, these data demonstrate that perturbations in cellular autophagy can affect both intracellular and surface levels of MR1 expression.

Autophagy regulates pre-existing pools of MR1 and at an early step of the trafficking pathway

Although the data presented thus far implicated the autophagy pathway in the regulation of MR1 function, it was unclear at which step of MR1 trafficking, from the ER to the plasma membrane, this regulation was occurring. MR1 transcripts were comparable between control and autophagy-depleted cells (Figure 5A), suggesting that this effect was not due to differences in the levels of mRNA. MR1 at the cell surface may be internalized and either degraded or recycled via an autophagic pathway as described for MHC Class 1. To address this point, we incubated control and autophagy-depleted cells with DMSO or Ac-6-FP overnight and then chased in ligand free media for up to 12 hours (Figure 5B). We found no difference between the cell lines in the rate of decline of surface MR1 over the 12 hour chase period. This indicates that MR1 already at the cell surface is not differentially regulated by autophagy. In contrast, differences in surface MR1 expression in control compared to Atg5 and Atg7-depleted cells was observed as early as 2 hours post ligand addition and become more pronounced at the 6 hour time point (Figure 5C). This indicates that regulation by autophagy occurs early in the trafficking of MR1, potentially before it reaches the plasma membrane. As MR1 is known to traffic via the Golgi to reach the plasma membrane, we

sought to determine the amounts of EndoH sensitive (pre-Golgi processed) to EndoH resistant (Golgi processed) MR1 forms in control and autophagy-deficient cells (Figure 5D). There appeared to be no difference in the ratio of EndoH sensitivity between the cell lines, demonstrating that MR1 is processed normally through the Golgi apparatus in the absence of autophagy. Lastly, we treated control and Atg-deficient cells with the protein synthesis inhibitor Cycloheximide (CHX) in the presence and absence of synthetic ligand to determine whether autophagy is regulating new or pre-existing MR1 protein populations (Figure 5E). As previously observed, there was an increase in surface MR1 levels in the Atg-depleted cells compared to the control in the presence of Ac-6-FP. Although treatment with CHX reduced surface MR1 expression in these cells to levels equivalent to the control cell line, the difference between the presence and absence of CHX was not statistically significant. Taken together, these data indicate that regulation of MR1 by autophagy is not dependent on new protein synthesis and is most likely occurring on pre-existing pools of MR1, the majority of which, in the absence of antigen, is contained within the ER.

Discussion

MR1 plays an essential role in presenting microbially derived antigens to MAIT cells and, as yet unidentified, antigens to MR1T and cancer-targeting T cells [11]. These functions are important in anti-microbial immunity and in the specific recognition of cancerous cells, respectively, as demonstrated by the high degree of sequence conservation of this protein [45]. Although functions for MR1 are becoming clearer, control of MR1 function by cellular co-factors remains to be fully characterized.

In this study, we were able to identify and validate several existing and newly identified MR1 interacting proteins. Some of these proteins have known roles in antigen presentation, particularly components of the PLC. This complex is more commonly associated with MHC Class I presentation and thus supports earlier and more recent findings that MR1 trafficking utilizes a similar pathway [1,21,26].

Although we were able to demonstrate interactions between MR1 and components of the PLC, including TAP2, this was only possible in the presence of *E. coli* and not at baseline or with 5-OP-RU alone, even with reduced incubation times to account for 5-OP-RU instability [7]. This is in contrast to the recent work of McWilliams et al, who performed a similar proteomics screen and were able to recover several of these interactions in the absence of ligand in C1R and Thp1 cells and in the presence of Ac-6-FP in C1R cells [26]. The reason for this discrepancy remains unclear but may reflect differences in experimental conditions, for example the type of tagged MR1 construct used, the level of overexpression, and the use of Ac-6-FP versus 5-OP-RU.

It is important to note that we also used a tagged overexpressed MR1 construct in order to obtain sufficient protein to perform the mass spectrometry analysis. We verified that the tag did not interfere with the correct folding of MR1 and that the construct was still functional [17]. We deliberately chose Thp1 cells to perform these experiments as they are natural APCs and thus the cellular components required

for MR1 antigen presentation are fully active and present at endogenous levels. Further, we used fixed bacteria as well as synthetic 5-OP-RU, as the ability of the chemically synthesized antigen to access the MR1 compartment may not be fully recapitulated under *in vivo* conditions. This experimental setup was validated by recovery of β2M as a major MR1 interacting protein, as it is essential for MR1 surface expression and MAIT cell activation. We were also able to verify the interaction of MR1 with previously unidentified proteins such as SEL1L and SQSTM1. However, other interactions could not be confirmed by co-immunoprecipitation, most notably with IL23A. This was a highly significant hit in the proteomics screen, and although this protein could be easily detected in cells, there was no association with MR1 in our system. IL23A may be more readily detectable in the conditions used for mass spectrometry and may not be amenable to analysis by co-immunoprecipitation, or it could be a false positive hit. Nonetheless, despite the proteomics screen results, we were unable to confirm an interaction between MR1 and IL23A.

The interaction between MR1 and SQSTM1 led us to investigate the role of autophagy in MR1 function in more detail. Autophagy associated proteins have recently been shown to control levels of MHC Class I on the surface of dendritic cells through the endocytosis mediated receptor AAK1. Inhibition of autophagy through knockout of Atg5 and Atg7 led to increased cell surface Class I expression and enhanced CD8+ T cell responses to viral infections [28]. We found that depletion of Atg5 and Atg7 in our experimental system led to greater MR1 on the surface of APCs which resulted in increased IFNγ production from MAIT cells when stimulated with either *E. coli* or 5-OP-RU. Total MR1 protein levels were also increased when cells were treated with the autophagy inhibitors 3MA and wortmannin, and the use of the late stage autophagy inhibitor bafilomycin resulted in an increase in surface MR1 levels in primary monocytes and Thp1 cells, although intracellular protein expression was not affected. Thus when the generation of autolysosomes is blocked, surface MR1 is able to accumulate, implicating autophagy mediated degradation in the regulation of MR1 protein levels.

It is important to note that although the effects relating to MR1 surface expression and activation of MAIT cells in autophagy deficient cells were small this is most likely a consequence of the highly controlled regulation of MR1 expression particularly at the cell surface. Generally only ligand bound MR1 is trafficked to the PM and even then the endogenous protein is very difficult to detect. In contrast, Class I and other MHC molecules shuttle between the ER and PM regardless of ligand availability. This suggests that the mechanism underlying the regulation of MR1 may not be the same as that observed for MHC Class I. In support of this, we found no evidence of an interaction between MR1 and AAK1 and surface MR1 was removed at the same rate in control and autophagy deficient cells, indicating that MR1 internalization was not affected by autophagy. Although MR1 surface levels increased quickly in Atg-depleted cells, processing and trafficking through the Golgi appeared to be equivalent to that seen in control cells. Treatment with CHX also had no clear effect on surface MR1 levels when autophagy was inhibited, indicating that MR1 reaching the plasma membrane in this condition was not dependent on new protein synthesis and instead it was existing populations of MR1 that were regulated by the autophagy pathway. In the absence of antigen, this population is mostly contained within the ER as has previously been reported [24,26]. In support of this argument, induction of autophagy through amino acid starvation led to a decrease in surface MR1 levels, which were dramatically elevated in the presence of

5-OP-RU. This shows that MR1 targeted for degradation can be rescued by the addition of antigen and implies that it is the population of unbound, but ligand receptive, MR1 that is regulated by autophagy. This regulation may occur through a process such as ER associated degradation (ERAD), a quality control system which removes misfolded or incompletely folded proteins from the ER in response to ER stress. Proteins targeted by ERAD are normally degraded via the ubiquitin-proteosome system (UPS) but in some circumstances may instead be degraded by the autophagy-lysosome system [46–48]. The two systems are also likely to be compensatory [47,49]. Consistent with this notion, SEL1L, a key component of mammalian ERAD [50], was found to interact with MR1 in our system and MR1 degradation at steady state does not appear to be proteasome dependent, albeit at early timepoints [25,27]. However, further work would be required to explore this link in more detail.

SQSTM1 was identified as an MR1 interacting partner in our proteomics screen, as well as in a similar screen performed in C1R cells [26]. It plays an essential role in the selective autophagy pathway as it facilitates the removal of ubiquitinated proteins as well as bacteria from cells via autophagosomes [38,44,51–53]. In the presence of *E.coli,* knockout of SQSTM1 did not affect MR1 surface expression but did increase antigen presentation to MAIT cells in nearly all clones tested. In our hands, stimulation of Thp1 cells with fixed bacteria led to changes in MR1 and SQSTM1 expression levels as well as the composition of the MR1 proteome, specifically the interaction between MR1 and SQSTM1, which was undetectable at baseline or in the presence of 5-OP-RU. Whether abrogation of this interaction, as would be the case in the knockout clones, leads to the observed phenotype of increased MAIT activation either directly or indirectly remains to be determined. However, the contrasting results observed in the presence of 5-OP-RU imply that this regulation may be quite nuanced. In this case, loss of SQSTM1 either reduced MR1 surface expression and MAIT activation or had no effect, implying that in certain circumstances, SQSTM1 may be required for efficient MR1 antigen presentation. This raises the intriguing possibility that cellular regulation of MR1 may be antigen specific, as has previously been suggested [16,17,23,37] Further studies are required to determine whether this specificity has a biological significance in response to different microbes, for example intracellular vs extracellular bacteria.

Aside from its role in selective autophagy, SQSTM1 is also involved in several other cellular pathways, including the Keap1-Nrf2, mTORC1 and NFkB signalling pathways which are important for the antioxidant response, nutrient sensing and inflammation respectively [40,54–56]. Its multiple protein domain organization facilitates binding to specific cellular proteins which, in turn, contribute to its effector functions [41,57] . It is entirely possible that the contrasting effects of SQSTM1 on MR1 function in response to different antigenic stimuli are mediated by different cellular processes, which may or may not involve autophagy. Further work would be required to define this mechanism in more detail. For instance, mutagenesis of the different SQSTM1 protein domains would indicate which are necessary for regulation of MR1.

The multiple non-autophagy functions of SQSTM1 may also help to explain the results observed with deletion of SQSTM1 and Atg5/Atg7 in the presence of *E.coli*, as although these had phenotypically

similar effects on MAIT activation they are likely to be mechanistically different. Depletion of the Atg proteins leads to an increase in SQSTM1 expression as it is itself regulated by autophagy [39]. This increase in SQSTM1 protein levels still resulted in increased MR1 surface levels and activation of MAIT cells, the same phenotype observed in SQSTM1-depleted cells. On the other hand, global inhibition of autophagy is likely affecting numerous cellular pathways and proteins, any one of which could be contributing to MR1 function indirectly. Targeted disruption of autophagosome degradation through the use of bafilomycin provides a more defined parameter in which to measure MR1 regulation but the use of chemical reagents can also be problematic due to non-specific binding to other cellular proteins. Therefore, although SQSTM1 and the Atg5 and Atg7 proteins are part of the same pathway, their effects on MR1 may be distinct and dependent on the cellular context. For example, regulation by SQSTM1 appears to be dependent on the source of the ligand, which is not the case when autophagy as a whole is inhibited. Future studies should aim to address this discrepancy and precisely define the mechanisms at play.

Overall, these data expand our understanding of the MR1 interacting protein network and highlight the identification of autophagy associated proteins as cellular mediators of MR1 activity. Further work will be required to better understand this regulation and the implications for both microbial control and recognition of cancerous cells.

Materials and Methods

Cell Culture: 293T and HeLa cells were cultured in DMEM and Thp1 and C1R cells were cultured in RPMI both supplemented with 10% fetal bovine serum and penicillin-streptomycin. Thp1 and HeLa cells stably expressing a carboxyl-terminal hemaglutinin (HA) tagged MR1 were generated by standard lentivirus mediated transduction, followed by puromycin selection. Thp1 and/or C1R cells stably expressing either control, Atg5, Atg7, β2M or SQSTM1 targeting guide RNAs were generated by standard lentivirus mediated transduction followed by selection with puromycin or GFP. Clonal cell populations were generated by limiting dilution.

CRISPR-Cas9: Guide RNAs were cloned into plentiCRISPRv2 (Addgene #52961) or plentiCRISPRv2GFP (Addgene #82416) using the BsmB1 restriction site. Cloned inserts were verified to be correct by sequencing. The sequences of the guide RNAs used in this study can be found in Table S2.

Fixed Bacteria: *E.coli* (DH5 alpha) were cultured overnight at 37°C in Luria broth (Sigma), washed in PBS and then fixed in 4% paraformaldehyde for 20 mins at room temperature. Bacteria were washed twice in PBS and resuspended in sterile filtered PBS. Bacteria were quantified as previously described [17] and added at a concentration of 30 bacteria per cell (bpc) unless otherwise stated.

Ligands: 5-OP-RU was synthesised in DMSO as previously reported [6,7], and used as a DMSO solution due to its much greater stability than in water, with care taken to minimize exposure time to water in cellular experiments. Ac-6-FP (Cayman Chemicals, 23303) was resuspended in DMSO and both synthetic ligands were used at a concentration of 10µM unless otherwise stated.

Autophagy Inhibitors: 5mM 3MA (Sigma, M9281) and 1µM Wortmannin (Sigma, 12338) were added to Thp1 or HeLa cells for 4 hours. For autophagy induction experiments, cells were washed in PBS and resuspended in EBSS media (Gibco) for 4 hours, with 100nM Bafilomycin (Sigma, 19-148) added for the final 2 hours.

Coimmunoprecipitation: $5x10^6$ Thp1 or Thp1.MR1.HA cells were incubated overnight (or 2 hours) with and without fixed *E.coli* or 5-OP-RU. Cells were harvested, washed in phosphate buffered saline (PBS) and resuspended in 500µL Lysis Buffer [0.5% NP40, 150 mM NaCl, 50 mM Tris-HCL(pH7.5), protease inhibitor (+ EDTA)] for 30 mins at 4°C with rotation. Lysates were cleared by centrifugation for 10 mins at 1000xg and then added to HA conjugated Dynabeads (ThermoFisher) for 2 hours at 4°C with rotation. The beads were washed 3 times, resuspended in loading buffer and proteins were eluted from the beads by boiling. Samples were run on 4-12% Tris-Glycine SDS-PAGE gradient gels (ThermoFisher Scientific) and resolved proteins were analyzed by immunoblotting using the following primary antibodies; anti-Atg5 (ab108327, Abcam), anti-Atg7 (8558, Cell Signalling), anti-AUP1 (35055, Cell Signalling), anti-Bag2 (ab79406, Abcam), anti-βactin (ab227387, Abcam), anti-β2M (ab75853, Abcam), anti-Calnexin ab22595, Abcam), anti-Calreticulin (ab92516, Abcam), anti-GAPDH (ab8245, Abcam), anti-HA (NB600-363, Novus Biologicals), anti-Hsp90 (sc-13119, Santa Cruz Biotechnology), anti-IL23 (ab45420, Abcam), anti-LC3B (ab51520, Abcam), anti-SEL1L (ab78298, Abcam), anti-SQSTM1 (ab109012, Abcam), anti-STING (ab181125, Abcam), anti-Tapasin (MABF249, Merck). Bound antibodies were visualized using appropriate horseradish peroxidase conjugated secondary antibodies and enhanced chemiluminscence. For EndoH experiments, following the final wash proteins were eluted in Glycoprotein Denaturing Buffer (NEB, P0702S) for 10 mins at 100°C and then resuspended in EndoH (NEB, P0702S) for 1.5 hours at 37°C. Samples were then prepared for immunoblotting as described above.

Immunofluorescence: Sub-confluent HeLa cell monolayers were seeded onto glass coverslips. Twenty-four hours later, cells were treated with the appropriate autophagy reagent, as described above, and then washed three times in PBS and fixed with 4% paraformaldehyde (Electron Microscopy Sciences) for 15 mins. Cells were permeabilized with 0.2% Triton X-100 and then blocked with NGB Buffer (50 mM NH4Cl, 1% goat serum, 1% bovine serum albumin) for 1 hour. Cells were then incubated with the indicated primary antibodies for 2 hours and the appropriate species specific Alexa Fluor 488 or 594 conjugated secondary antibody for 1 hour. Coverslips were mounted onto slides using Diamond Anti-Fade Mounting Reagent Plus DAPI (ThermoFisher). Images are z-stack projections acquired on an Olympus FV1000 laser scanning confocal microscope and processed using FIJI software.

Proteomics/Mass Spec: 10^8 Thp1 and Thp1-MR1 cells per condition were incubated with fixed *E.coli* overnight. Cells were washed and resuspended in Lysis Buffer (as above) and incubated for 30 mins at

4°C. Lysates were cleared by centrifugation for 10 mins at 1000xg and added to HA conjugated Dynabeads for 2 hours with rotation. The beads were washed 4 times in Wash Buffer (with the final wash without detergent) and proteins were eluted from the beads using 2% acetic acid. Eluted samples were trypsin digested and run on an liquid chromatography tandem MS (LC-MS/MS) system. Peptides were resuspended in 5% formic acid and 5% DMSO and then trapped on a C18 PepMap100 pre-column (300µm i.d. x 5mm, 100 Å, Thermo Fisher Scientific) using solvent A (0.1% Formic Acid in water) at a pressure of 500 bar and separated on an Ultimate 3000 UHPLC system (Thermo Fischer Scientific) coupled to a QExactive mass spectrometer (Thermo Fischer Scientific). The peptides were separated on an in-house packed analytical column (360µm x 75µm i.d. packed with ReproSil-Pur 120 C18-AQ, 1.9µm, 120 Å, Dr.Maisch GmbH) and then electrosprayed directly into an QExactive mass spectrometer (Thermo Fischer Scientific) through an EASY-Spray nano-electrospray ion source (Thermo Fischer Scientific) using a linear gradient (length: 60 minutes, 15% to 35% solvent B (0.1% formic acid in acetonitrile), flow rate: 200 nL/min). The raw data was acquired on the mass spectrometer in a data-dependent mode (DDA). Full scan MS spectra were acquired in the Orbitrap (scan range 350-2000 m/z, resolution 70000, AGC target 3e6, maximum injection time 50 ms). After the MS scans, the 20 most intense peaks were selected for HCD fragmentation at 30% of normalized collision energy. HCD spectra were also acquired in the Orbitrap (resolution 17500, AGC target 5e4, maximum injection time 120 ms) with first fixed mass at 180 m/z. The raw data files generated were processed using MaxQuant (Version 1.5.0.35), integrated with the Andromeda search engine as previously described [1,2]. For protein groups identification, peak lists were searched against human database (Swiss--Prot, version 04/13) as well as a list of common contaminants by Andromeda. Trypsin with a maximum number of missed cleavages of 2 was chosen. Acteylation (Protein N—term) and Oxidation (M) were selected as variable modifications while Carbamidomethylation (C) was set as a fixed modification. Protein and PSM false discovery rate (FDR) were set at 0.01.

Flow Cytometry: For the MAIT cell activation assay, Thp1 cells were incubated with or without fixed *E.coli* or 5-OP-RU overnight. PBMCs from healthy donors (NHS Blood Bank, Oxford) were thawed and CD8+ T cells positively enriched using CD8 microbeads (Miltenyi Biotech) as per the manufacturer's instructions. CD8+ T cells were incubated with Thp1 cells at a 1:1 ratio for 5 hours, with Brefeldin A added for the final 4 hours. Cells were washed with PBS and stained with Live/Dead Fixable Near IR dye (Invitrogen) for 20 mins at room temperature. Cells were washed and fixed with 2% paraformaldehyde for 20 mins at 4°C. Cells were then washed twice in 1X Permeabilization Buffer (eBioscience) and stained with the following antibodies; CD3-Pe-Cy7 (25-0038-42, eBioScience), CD4-Viogreen (130-113-230, Miltenyi Biotech), CD8-eFluor450 (8-0086-42, Invitrogen), CD161-PE (130-113-593, Miltenyi Biotech), Vα7.2-APC (351708, Biolegend) and IFNγ-PerCpCy5.5 (45-7319-42, eBioScience). Cells were incubated for 25 mins at room temperature, washed and acquired on a MACSQuant Cytometer (Miltenyi Biotech).

For MR1 surface staining, cells were incubated with or without fixed *E.coli*, 5-OP-RU or Ac-6-FP overnight or for up to 6 hours. For cyclohexamide (CHX) experiments, cells were first incubated with 10µM CHX (Merck) for 1 hour before the addition of ligand for 6 hours. Cells were washed with PBS and then incubated with Human TruStain FcX Blocking Solution (Biolegend) for 10 mins. Cells were

stained with MR1-PE (361106, Biolegend) or a matched isotype control (400214, Biolegend) antibody for 20 mins at room temperature. Cells were fixed in 2% paraformaldehyde for 20 mins at 4°C, washed in PBS and acquired on a MACSQuant. All data were analyzed using FlowJo version 10 software. For MHC-I surface staining, cells were stained with an HLA-ABC-FITC (11-9983-42, eBioScience) antibody.
For monocyte staining, PBMCs from healthy donors were first CD3 depleted using CD3 microbeads (Milteny Biotech) as per the manufacturer's instructions and then stained using CD14-FITC (301804, Biolegend), CD16-PeCy7 (980110, Biolegend) and HLADR-BV41 (307636, Biolegend).

qRT-PCR: RNA was extracted from Thp1 cells using an RNeasy mini kit (Qiagen) as per the manufacturer's instructions and equal volumes reverse transcribed using the appSCRIPT cDNA synthesis kit (Appleton Woods). qPCRs were performed in triplicate using Universal ProbeLibrary probes (Roche) on a LightCycler 480 machine (Roche). Results were normalized to the housekeeping genes GAPDH and HRPT. The sequences of the primers used can be found in Table S2.

Statistical Analysis: Statistical significance was calculated by either a one or two way ANOVA or a 2 tailed paired t-test, as indicated in the figure legends, using GraphPad Prism software (version 7).

Data availability

The proteomics dataset generated during the current study has been deposited to the ProteomeXchange Consortium via the MassIVE repository with the dataset identifier MSV000089910 and is available here: https://massive.ucsd.edu/ProteoSAFe/private-dataset.jsp?task=7f9ad709f11a4ba88ea03dc43050a17a.

Acknowledgements

We wish to thank the Advanced Proteomics Facility, University of Oxford, and the Micron Bioimaging Facility, University of Oxford, for their assistance with this work. We would also like to thank Dr. Matthew Edmans for careful reading of the manuscript and Drs Lucy Garner, Carl-Philipp Hackstein and Narayan Ramamurthy for helpful discussions. D.P.F. is supported by funding from the National Health and Medical Research Council (2009551), and the National Institute of Allergy and Infectious Diseases of the National Institutes of Health (R01AI148407NIH). P.K. is supported by funding from the Wellcome Trust (109965MA and 222426/Z/21/Z).

Author contributions

Conceptualization and Methodology, P.P., J.U. and P.K.; Investigation, P.P. and S.H.; Formal Analysis, P.P., S.H., E.M.; Resources, J.U., J.Y.M.K. and D.P.F.; Writing-Original Draft, P.P.; Writing-Review and Editing, P.P., J.U., J.Y.M.K., D.P.F. and P.K.; Supervision and Funding Acquisition, P.K.

Competing interests

The authors declare no competing interests

References

1. Treiner, E. *et al.* Selection of evolutionarily conserved mucosal-associated invariant T cells by MR1. *Nature* **422**, 164–169 (2003).

2. Dusseaux, M. *et al.* Human MAIT cells are xenobiotic-resistant, tissue-targeted, CD161 hi IL-17-secreting T cells. *Blood* **117**, 1250–1259 (2011).

3. Kurioka, A. *et al.* MAIT cells are licensed through granzyme exchange to kill bacterially sensitized targets. *Mucosal Immunology* **8**, 429–440 (2015).

4. Billerbeck, E. *et al.* Analysis of CD161 expression on human CD8+ T cells defines a distinct functional subset with tissue-homing properties. *Proceedings of the National Academy of Sciences of the United States of America* **107**, 3006–3011 (2010).

5. Corbett, A. J. *et al.* T-cell activation by transitory neo-antigens derived from distinct microbial pathways. *Nature* **509**, 361–365 (2014).

6. Mak, J. Y. W., Liu, L. & Fairlie, D. P. Chemical Modulators of Mucosal Associated Invariant T Cells. *Accounts of Chemical Research* **54**, 3462–3475 (2021).

7. Mak, J. Y. W. *et al.* Stabilizing short-lived Schiff base derivatives of 5-aminouracils that activate mucosal-associated invariant T cells. *Nature Communications* **8**, (2017).

8. Kjer-Nielsen, L. *et al.* MR1 presents microbial vitamin B metabolites to MAIT cells. *Nature* **491**, 717–723 (2012).

9. Lepore, M. *et al.* Functionally diverse human T cells recognize non-microbial antigens presented by MR1. *eLife* **6**, (2017).

10. Crowther, M. D. *et al.* Genome-wide CRISPR–Cas9 screening reveals ubiquitous T cell cancer targeting via the monomorphic MHC class I-related protein MR1. *Nature Immunology* **21**, 178–185 (2020).

11. Corbett, A. J., Awad, W., Wang, H. & Chen, Z. Antigen Recognition by MR1-Reactive T Cells; MAIT Cells, Metabolites, and Remaining Mysteries. *Frontiers in Immunology* vol. 11 Preprint at https://doi.org/10.3389/fimmu.2020.01961 (2020).

12. Kjer-Nielsen, L. *et al.* An overview on the identification of MAIT cell antigens. *Immunology and Cell Biology* vol. 96 573–587 Preprint at https://doi.org/10.1111/imcb.12057 (2018).

13. Lamichhane, R. & Ussher, J. E. Expression and trafficking of MR1. *Immunology* vol. 151 270–279 Preprint at https://doi.org/10.1111/imm.12744 (2017).

14. Huang, S. *et al.* MR1 uses an endocytic pathway to activate mucosal-associated invariant T cells. *Journal of Experimental Medicine* **205**, 1201–1211 (2008).

15. Chua, W.-J. *et al.* Endogenous MHC-Related Protein 1 Is Transiently Expressed on the Plasma Membrane in a Conformation That Activates Mucosal-Associated Invariant T Cells. *The Journal of Immunology* **186**, 4744–4750 (2011).

16. Kulicke, C., Karamooz, E., Lewinsohn, D. & Harriff, M. Covering All the Bases: Complementary MR1 Antigen Presentation Pathways Sample Diverse Antigens and Intracellular Compartments. *Frontiers in Immunology* vol. 11 Preprint at https://doi.org/10.3389/fimmu.2020.02034 (2020).

17. Ussher, J. E. *et al.* TLR signaling in human antigen-presenting cells regulates MR1-dependent activation of MAIT cells. *European Journal of Immunology* **46**, 1600–1614 (2016).

18. Liu, J. & Brutkiewicz, R. R. The Toll-like receptor 9 signalling pathway regulates MR1-mediated bacterial antigen presentation in B cells. *Immunology* **152**, 232–242 (2017).

19. McWilliam, H. E. G. *et al.* The intracellular pathway for the presentation of Vitamin B-related antigens by the antigen-presenting molecule MR1. *Nature Immunology* **17**, 531–537 (2016).

20. Yamaguchi, H., Hirai, M., Kurosawa, Y. & Hashimoto, K. A highly conserved major histocompatibility complex class I-related gene in mammals. *Biochemical and Biophysical Research Communications* **238**, 697–702 (1997).

21. Miley, M. J. *et al.* Biochemical Features of the MHC-Related Protein 1 Consistent with an Immunological Function. *The Journal of Immunology* **170**, 6090–6098 (2003).

22. Aldemir, H. Novel MHC class I-related molecule MR1 affects MHC class I expression in 293T cells. *Biochemical and Biophysical Research Communications* **366**, 328–334 (2008).

23. Harriff, M. J. *et al.* Endosomal MR1 Trafficking Plays a Key Role in Presentation of Mycobacterium tuberculosis Ligands to MAIT Cells. *PLoS Pathogens* **12**, (2016).

24. McWilliam, H. E. G., Birkinshaw, R. W., Villadangos, J. A., McCluskey, J. & Rossjohn, J. MR1 presentation of vitamin B-based metabolite ligands. *Current Opinion in Immunology* vol. 34 28–34 Preprint at https://doi.org/10.1016/j.coi.2014.12.004 (2015).

25. Abós, B. *et al.* Human MR1 expression on the cell surface is acid sensitive, proteasome independent and increases after culturing at 26°C. *Biochemical and Biophysical Research Communications* **411**, 632–636 (2011).

26. McWilliam, H. E. G. *et al.* Endoplasmic reticulum chaperones stabilize ligand-receptive MR1 molecules for efficient presentation of metabolite antigens. *Proceedings of the National Academy of Sciences of the United States of America* **117**, 24974–24985 (2020).

27. Kulicke, C. A. *et al.* The P5-type ATPase ATP13A1 modulates major histocompatibility complex I-related protein 1 (MR1)-mediated antigen presentation. *Journal of Biological Chemistry* **298**, 101542 (2022).

28. Loi, M. *et al.* Macroautophagy Proteins Control MHC Class I Levels on Dendritic Cells and Shape Anti-viral CD8+ T Cell Responses. *Cell Reports* **15**, 1076–1087 (2016).

29. Xie, Z. & Klionsky, D. J. Autophagosome formation: Core machinery and adaptations. *Nature Cell Biology* vol. 9 1102–1109 Preprint at https://doi.org/10.1038/ncb1007-1102 (2007).

30. Mizushima, N. Autophagy: Process and function. *Genes and Development* vol. 21 2861–2873 Preprint at https://doi.org/10.1101/gad.1599207 (2007).

31. Glick, D., Barth, S. & Macleod, K. F. Autophagy: Cellular and molecular mechanisms. *Journal of Pathology* vol. 221 3–12 Preprint at https://doi.org/10.1002/path.2697 (2010).

32. Simonsen, A. & Tooze, S. A. Coordination of membrane events during autophagy by multiple class III PI3-kinase complexes. *Journal of Cell Biology* vol. 186 773–782 Preprint at https://doi.org/10.1083/jcb.200907014 (2009).

33. Mizushima, N., Yoshimori, T. & Ohsumi, Y. The role of atg proteins in autophagosome formation. *Annual Review of Cell and Developmental Biology* **27**, 107–132 (2011).

34. Cua, D. J. *et al.* Interleukin-23 rather than interleukin-12 is the critical cytokine for autoimmune inflammation of the brain. *Nature* **421**, 744–748 (2003).

35. Langrish, C. L. *et al.* IL-23 drives a pathogenic T cell population that induces autoimmune inflammation. *Journal of Experimental Medicine* **201**, 233–240 (2005).

36. Trinchieri, G., Pflanz, S. & Kastelein, R. A. The IL-12 family of heterodimeric cytokines: New players in the regulation of T cell responses. *Immunity* vol. 19 641–644 Preprint at https://doi.org/10.1016/S1074-7613(03)00296-6 (2003).

37. Karamooz, E., Harriff, M. J., Narayanan, G. A., Worley, A. & Lewinsohn, D. M. MR1 recycling and blockade of endosomal trafficking reveal distinguishable antigen presentation pathways between Mycobacterium tuberculosis infection and exogenously delivered antigens. *Scientific Reports* **9**, (2019).

38. Pankiv, S. *et al.* p62/SQSTM1 binds directly to Atg8/LC3 to facilitate degradation of ubiquitinated protein aggregates by autophagy*[S]. *Journal of Biological Chemistry* **282**, 24131–24145 (2007).

39. Komatsu, M. *et al.* Homeostatic Levels of p62 Control Cytoplasmic Inclusion Body Formation in Autophagy-Deficient Mice. *Cell* **131**, 1149–1163 (2007).

40. Katsuragi, Y., Ichimura, Y. & Komatsu, M. P62/SQSTM1 functions as a signaling hub and an autophagy adaptor. *FEBS Journal* vol. 282 4672–4678 Preprint at https://doi.org/10.1111/febs.13540 (2015).

41. Komatsu, M., Kageyama, S. & Ichimura, Y. P62/SQSTM1/A170: Physiology and pathology. *Pharmacological Research* vol. 66 457–462 Preprint at https://doi.org/10.1016/j.phrs.2012.07.004 (2012).

42. Kirkin, V. *et al.* A Role for NBR1 in Autophagosomal Degradation of Ubiquitinated Substrates. *Molecular Cell* **33**, 505–516 (2009).

43. Klionsky, D. J. *et al.* Guidelines for the use and interpretation of assays for monitoring autophagy (4th edition)1. *Autophagy* vol. 17 1–382 Preprint at https://doi.org/10.1080/15548627.2020.1797280 (2021).

44. Bjørkøy, G. *et al.* p62/SQSTM1 forms protein aggregates degraded by autophagy and has a protective effect on huntingtin-induced cell death. *Journal of Cell Biology* **171**, 603–614 (2005).

45. Huang, S. *et al.* Evidence for MR1 antigen presentation to mucosal-associated invariant T cells. *Journal of Biological Chemistry* **280**, 21183–21193 (2005).

46. Rashid, H. O., Yadav, R. K., Kim, H. R. & Chae, H. J. ER stress: Autophagy induction, inhibition and selection. *Autophagy* **11**, 1956–1977 (2015).

47. Kocaturk, N. M. & Gozuacik, D. Crosstalk between mammalian autophagy and the ubiquitin-proteasome system. *Frontiers in Cell and Developmental Biology* vol. 6 Preprint at https://doi.org/10.3389/fcell.2018.00128 (2018).

48. Houck, S. A. *et al.* Quality Control Autophagy Degrades Soluble ERAD-Resistant Conformers of the Misfolded Membrane Protein GnRHR. *Molecular Cell* **54**, 166–179 (2014).

49. Demishtein, A. *et al.* SQSTM1/p62-mediated autophagy compensates for loss of proteasome polyubiquitin recruiting capacity. *Autophagy* **13**, 1697–1708 (2017).

50. Sun, S. *et al.* Sel1L is indispensable for mammalian endoplasmic reticulum-associated degradation, endoplasmic reticulum homeostasis, and survival. *Proceedings of the National Academy of Sciences of the United States of America* **111**, (2014).

51. Kim, P. K., Hailey, D. W., Mullen, R. T. & Lippincott-Schwartz, J. Ubiquitin signals autophagic degradation of cytosolic proteins and peroxisomes. *Proceedings of the National Academy of Sciences of the United States of America* **105**, 20567–20574 (2008).

52. Dupont, N. *et al.* Shigella Phagocytic Vacuolar Membrane Remnants Participate in the Cellular Response to Pathogen Invasion and Are Regulated by Autophagy. *Cell Host and Microbe* **6**, 137–149 (2009).

53. Zheng, Y. T. *et al.* The Adaptor Protein p62/SQSTM1 Targets Invading Bacteria to the Autophagy Pathway. *The Journal of Immunology* **183**, 5909–5916 (2009).

54. Duran, A. *et al.* P62 Is a Key Regulator of Nutrient Sensing in the mTORC1 Pathway. *Molecular Cell* **44**, 134–146 (2011).

55. Sanz, L., Sanchez, P., Lallena, M. J., Diaz-Meco, M. T. & Moscat, J. The interaction of p62 with RIP links the atypical PKCs to NF-κB activation. *EMBO Journal* **18**, 3044–3053 (1999).

56. Komatsu, M. *et al.* The selective autophagy substrate p62 activates the stress responsive transcription factor Nrf2 through inactivation of Keap1. *Nature Cell Biology* **12**, 213–223 (2010).

57. Lamark, T., Svenning, S. & Johansen, T. Regulation of selective autophagy: The p62/SQSTM1 paradigm. *Essays in Biochemistry* vol. 61 609–624 Preprint at https://doi.org/10.1042/EBC20170035 (2017).

Figure Legends

Figure 1: A proteomics screen to define MR1 associated proteins during antigen presentation. A. Thp1 and Thp1.MR1.HA cells were incubated with fixed *E.coli* overnight and lysed in 0.5% NP40. MR1 was immunoprecipitated from lysates using a HA antibody conjugated to magnetic beads. Bound proteins were eluted, trypsin digested and analyzed using LC/LC-MS. Significantly enriched proteins in the presence of MR1 are shown in the top right quadrant. Components of the peptide loading complex are highlighted in black and other proteins of interest are highlighted in red. Data were combined from 3 independent replicates and were analyzed using MAXQuant software. B. Pathways analysis of the most highly enriched genes in the MR1 fraction. C. Thp1 and Thp1-MR1.HA cells were incubated with fixed *E.coli* overnight and then lysed in 0.5% NP40. MR1 was immunoprecipitated using a HA antibody conjugated to magnetic beads. Immunoprecipitates were analyzed by western blot and probed with the indicated antibodies. D. As for C but cells were incubated with 5-OP-RU overnight. Data in C and D are representative of at least 3 independent experiments. The position of molecular weight marker bands (kDa) are indicated to the left of the immunoblots.

Figure 2: Knock-out of the autophagy adaptor protein SQSTM1 leads to increased MAIT cell activation in the presence of *E.coli*. A. Thp1 cells were transduced with gRNAs directed against β2M (left) and SQSTM1 (right). Single cell clones were established by limiting dilution and knockout confirmed by western blot by probing with the indicated antibodies. The position of molecular weight marker bands (kDa) are indicated to the left of the immunoblots. B. Knockout clones for β2M (B1 and B6) and SQSTM1 (S1, S2, S3 and S4) produced in A were incubated with DMSO, fixed *E.coli*, 5-OP-RU or Ac-6-FP overnight and then stained for surface MR1 expression. Representative histograms displaying geometric MFIs are shown. C. Quantification of data as described in B. Displayed are means from 3 independent experiments ± SD. D. Knockout clones for β2M and SQSTM1 as described in A were incubated with either fixed *E.coli* (left) or 5-OP-RU (right) overnight. Cells were incubated with CD8+ enriched T cells from healthy donors for 5 hours with Brefeldin A added for the final 4 hours. % IFNγ production ± SD from CD161++Vα7.2+ cells was determined by FACS. For C and D, statistical significance was calculated using a one-way ANOVA, * = $p < 0.05$, ns = $p > 0.05$.

Figure 3: Depletion of Atg5 and Atg7 increases MAIT cell activation. A. Thp1 cells were transduced with gRNAs targeting Atg5 (left) or Atg7 (right). Protein depletion was analyzed by western blot. The position of molecular weight marker bands (kDa) are indicated to the left of the immunoblots. B. Atg5 (top) and Atg7 (bottom) depleted cell lines as produced in A were incubated with DMSO, fixed *E.coli* or 5-OP-RU overnight and then stained for MR1 surface expression. A representative histogram is shown on the left, with geometric MFIs displayed, and the average ± SD of at least 3 independent experiments is shown in the bar plots on the right. Cells described in A were incubated with *E.coli* (C) or 5-OP-RU (D) overnight and analyzed for MAIT cell IFNγ production as described in Figure 2D. For B, C and D statistical significance was calculated using a one-way ANOVA, * = $p < 0.05$.

Figure 4: Manipulation of autophagy alters MR1 intracellular and surface expression levels. Thp1.MR1.HA cells were incubated with DMSO, 100nM bafilomycin (Baf), 5mM 3MA, 1μM

wortmannin (Wort), EBSS or EBSS + 100nM bafilomycin (EBSS+Baf) for 4 hours (bafilomycin was added for the final 2 hours) and then lysed. Cell lysates were probed with the indicated antibodies by western blot. Image is representative of 2 independent experiments. The position of molecular weight marker bands (kDa) is indicated to the left of the immunoblots and the LC3-I (I) and LC3-II (II) bands are indicated on the right. B. HeLa cells expressing MR1.HA were grown on coverslips and incubated in normal media +/- bafilomycin, 3MA or wortmannin and EBSS media +/- bafilomycin for 4 hours with bafilomycin added for the final 2 hours. Cells were fixed and then permeabilized with 0.1% TritonX-100 and stained with anti-HA (rat) and anti-SQSTM1 (rabbit) primary antibodies and species specific Alexa Fluor conjugated secondary antibodies. Images are representative of at least 3 independent experiments using HeLa cells expressing MR1.HA or MR1.GFP. Scale bar = 10µm. C. Thp1.MR1.HA cells (top) or primary human monocytes (bottom) were pre-incubated (right) or not (left) with 5-OP-RU for 2 hours and then treated with autophagy reagents as in A and stained for surface MR1 expression. Displayed is the average ± SD from 3 independent experiments (top) or from 4 healthy blood donors (bottom). Statistical significance was calculated using a two-way ANOVA, * = $p < 0.05$. ns = $p > 0.05$.

Figure 5: Autophagy regulates pre-existing pools of MR1 and at an early step of the trafficking pathway. A. MR1 transcript levels were measured in Atg5 and Atg7 depleted cells and fold change in expression compared to the control cell line was calculated. ΔΔCT values were normalized to the housekeeping genes, GAPDH and HRPT. B. Control or Atg5 (5.3) and Atg7 (7.2) depleted cell lines were incubated overnight with either DMSO or Ac-6-FP. Cells were washed and incubated in ligand free media for up to 12 hours. Surface MR1 levels were measured at the indicated timepoints and are displayed as % expression compared to the 0 hour timepoint (beginning of the chase) which is set at 100%. Data is the mean of 2 independent experiments. C. Control or indicated Atg5 (5.2 and 5.3) and Atg7 (7.1 and 7.2) depleted cell lines were incubated with Ac-6-FP and surface MR1 levels were measured every hour for up to 6 hours. Displayed are the average gMFIs ± SD from 3 independent experiments. D. Thp1.MR1.HA control or Atg5 (5.3) or Atg7 (7.2) depleted cell lines were incubated with DMSO or Ac-6-FP overnight. Cells were lysed and MR1 immunoprecipitated using a HA antibody conjugated to magnetic beads. Samples were treated or not with EndoH for 1.5 hours and analyzed by western blot by probing with the indicated antibodies. Input samples are shown as a control below. The position of the molecular weight marker bands (kDa) are indicated to the left of the immunoblots and the MR1 EndoH resistant (R) and senstitive (S) bands are indicated on the right. Image is representative of 4 independent experiments with the quantification from all immunoblots shown in the bar plot below. Data is presented as the average ratio of S/R ± SD for the EndoH treated samples only. E. Control or Atg5 (5.3) and Atg7 (7.2) depleted cell lines were incubated with 20µM cycloheximide (CHX) for 7 hours, with DMSO or Ac-6-FP added after the 1st hour. Cells were stained for MR1 surface expression and displayed is the average gMFI ± SD from 3 independent experiments. Statistical significance was analyzed using a two-way ANOVA, ns = $p > 0.05$.

Figure 1

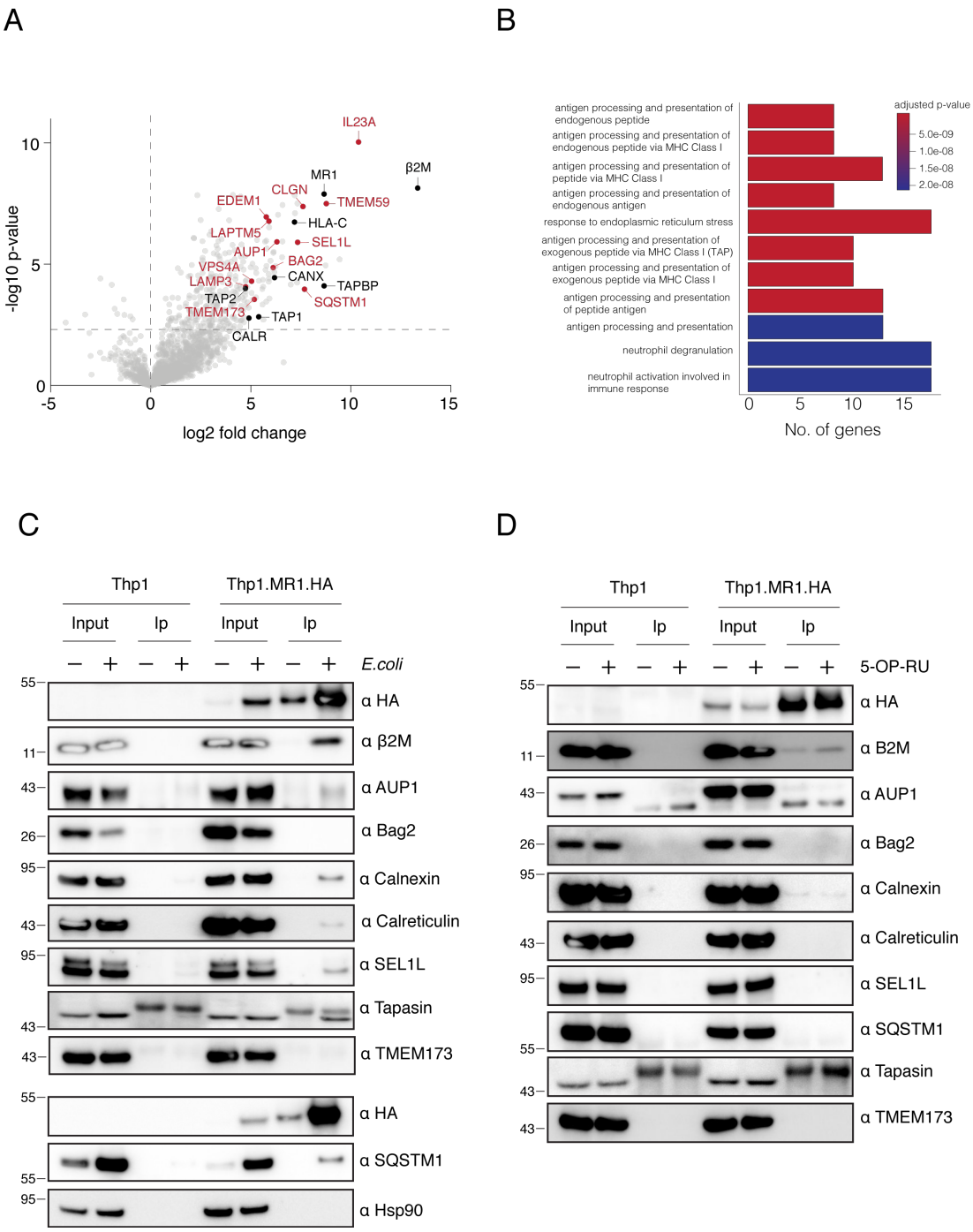
A
IL23A
β2M
MR1
CLGN
EDEM1
TMEM59
HLA-C
LAPTM5
SEL1L
AUP1
BAG2
VPS4A
CANX
LAMP3
TAPBP
TAP2
SQSTM1
TMEM173
TAP1
CALR
-log10 p-value
log2 fold change
B
antigen processing and presentation of endogenous peptide
antigen processing and presentation of endogenous peptide via MHC Class I
antigen processing and presentation of peptide via MHC Class I
antigen processing and presentation of endogenous antigen
response to endoplasmic reticulum stress
antigen processing and presentation of exogenous peptide via MHC Class I (TAP)
antigen processing and presentation of exogenous peptide via MHC Class I
antigen processing and presentation of peptide antigen
antigen processing and presentation
neutrophil degranulation
neutrophil activation involved in immune response
adjusted p-value
5.0e-09
1.0e-08
1.5e-08
2.0e-08
No. of genes
C
Thp1
Thp1.MR1.HA
Input
Ip
E.coli
α HA
α β2M
α AUP1
α Bag2
α Calnexin
α Calreticulin
α SEL1L
α Tapasin
α TMEM173
α SQSTM1
α Hsp90
D
5-OP-RU
α B2M

Figure 2

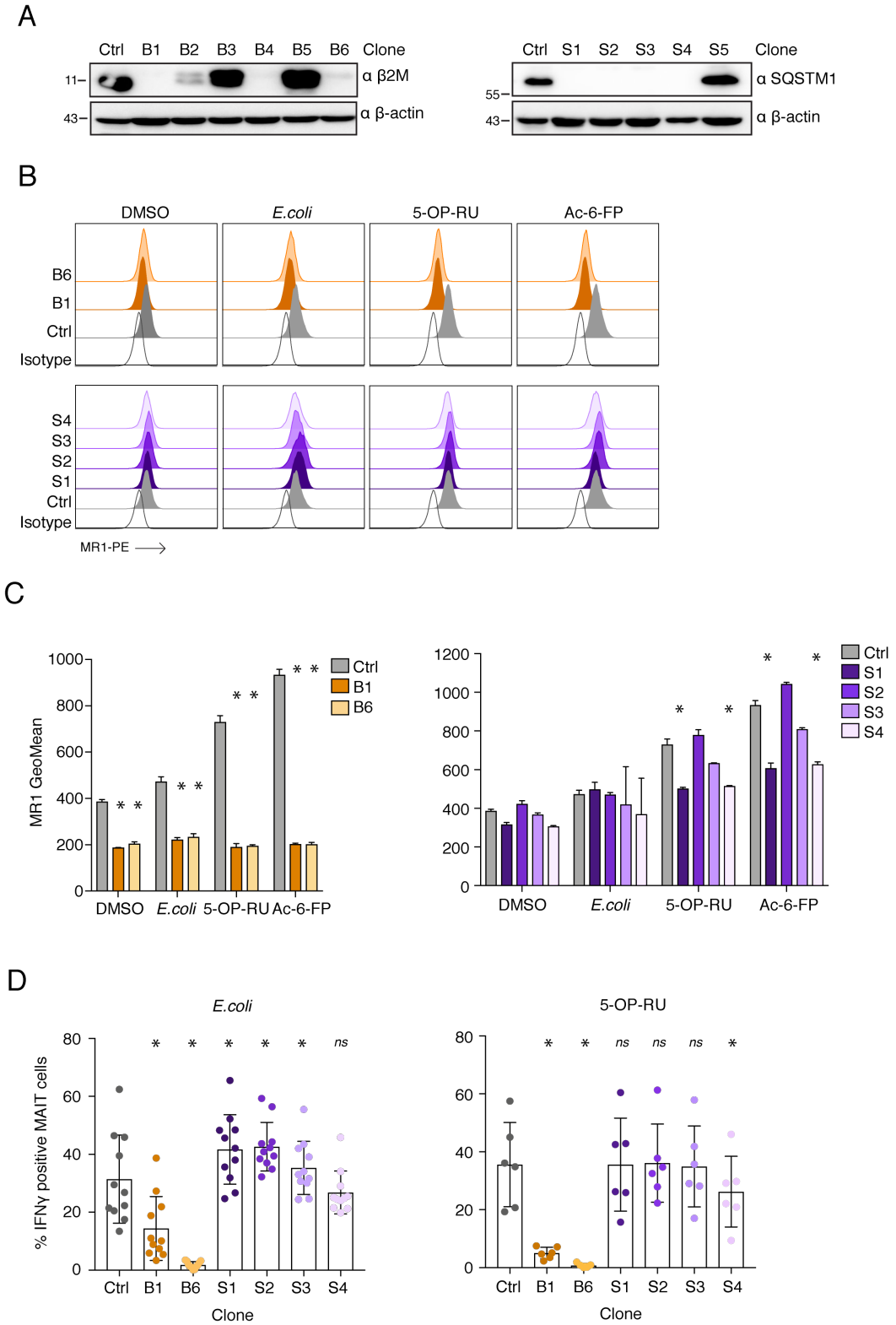
A
Ctrl B1 B2 B3 B4 B5 B6 Clone
11–
α β2M
43–
α β-actin
Ctrl S1 S2 S3 S4 S5 Clone
55–
α SQSTM1
43–
α β-actin
B
DMSO
E.coli
5-OP-RU
Ac-6-FP
B6
B1
Ctrl
Isotype
S4
S3
S2
S1
Ctrl
Isotype
MR1-PE
C
MR1 GeoMean
Ctrl
B1
B6
DMSO
E.coli
5-OP-RU
Ac-6-FP
Ctrl
S1
S2
S3
S4
D
E.coli
5-OP-RU
% IFNγ positive MAIT cells
Ctrl B1 B6 S1 S2 S3 S4
Clone
ns

Figure 3

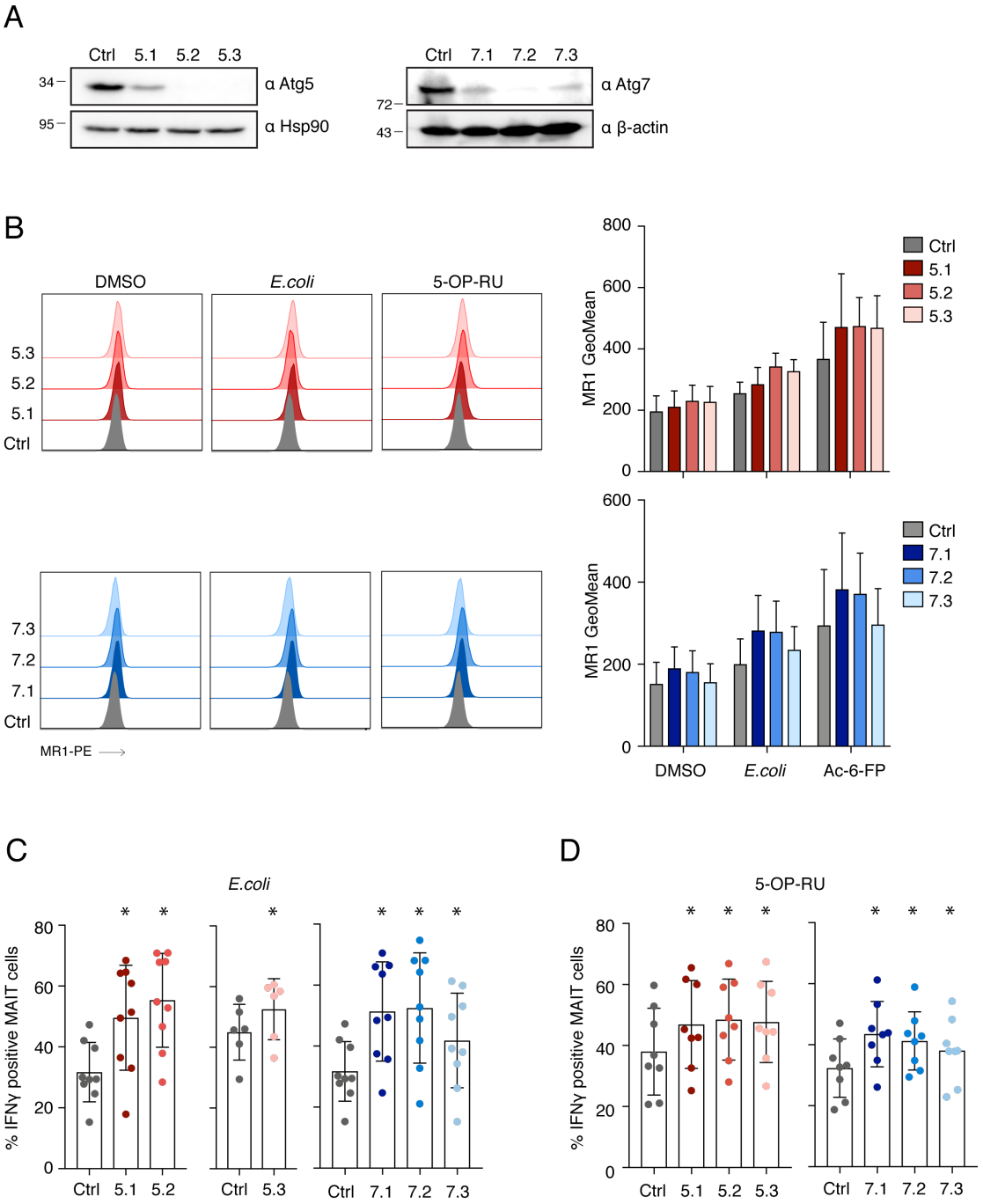
A
Ctrl 5.1 5.2 5.3
34
95
α Atg5
α Hsp90
Ctrl 7.1 7.2 7.3
72
43
α Atg7
α β-actin
B
DMSO
E.coli
5-OP-RU
5.3
5.2
5.1
Ctrl
7.3
7.2
7.1
Ctrl
MR1-PE
MR1 GeoMean
Ctrl
5.1
5.2
5.3
7.1
7.2
7.3
DMSO
E.coli
Ac-6-FP
C
E.coli
% IFNγ positive MAIT cells
Ctrl 5.1 5.2
Ctrl 5.3
Ctrl 7.1 7.2 7.3
D
5-OP-RU
Ctrl 5.1 5.2 5.3
Ctrl 7.1 7.2 7.3

Figure 4

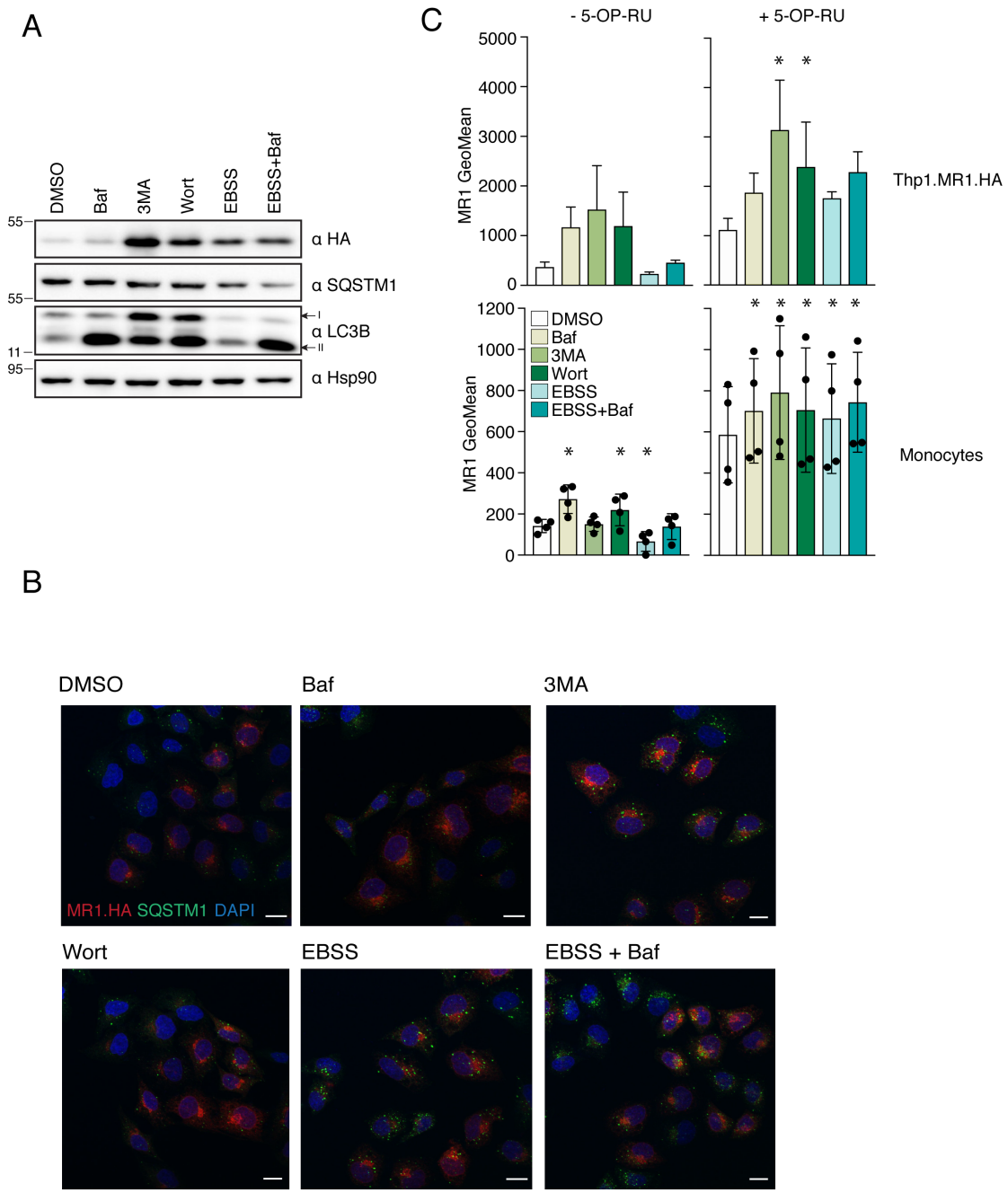
A
DMSO
Baf
3MA
Wort
EBSS
EBSS+Baf
55
α HA
α SQSTM1
55
I
α LC3B
II
11
95
α Hsp90
C
- 5-OP-RU
+ 5-OP-RU
MR1 GeoMean
Thp1.MR1.HA
DMSO
Baf
3MA
Wort
EBSS
EBSS+Baf
Monocytes
B
DMSO
Baf
3MA
MR1.HA SQSTM1 DAPI
Wort
EBSS
EBSS + Baf

Figure 5

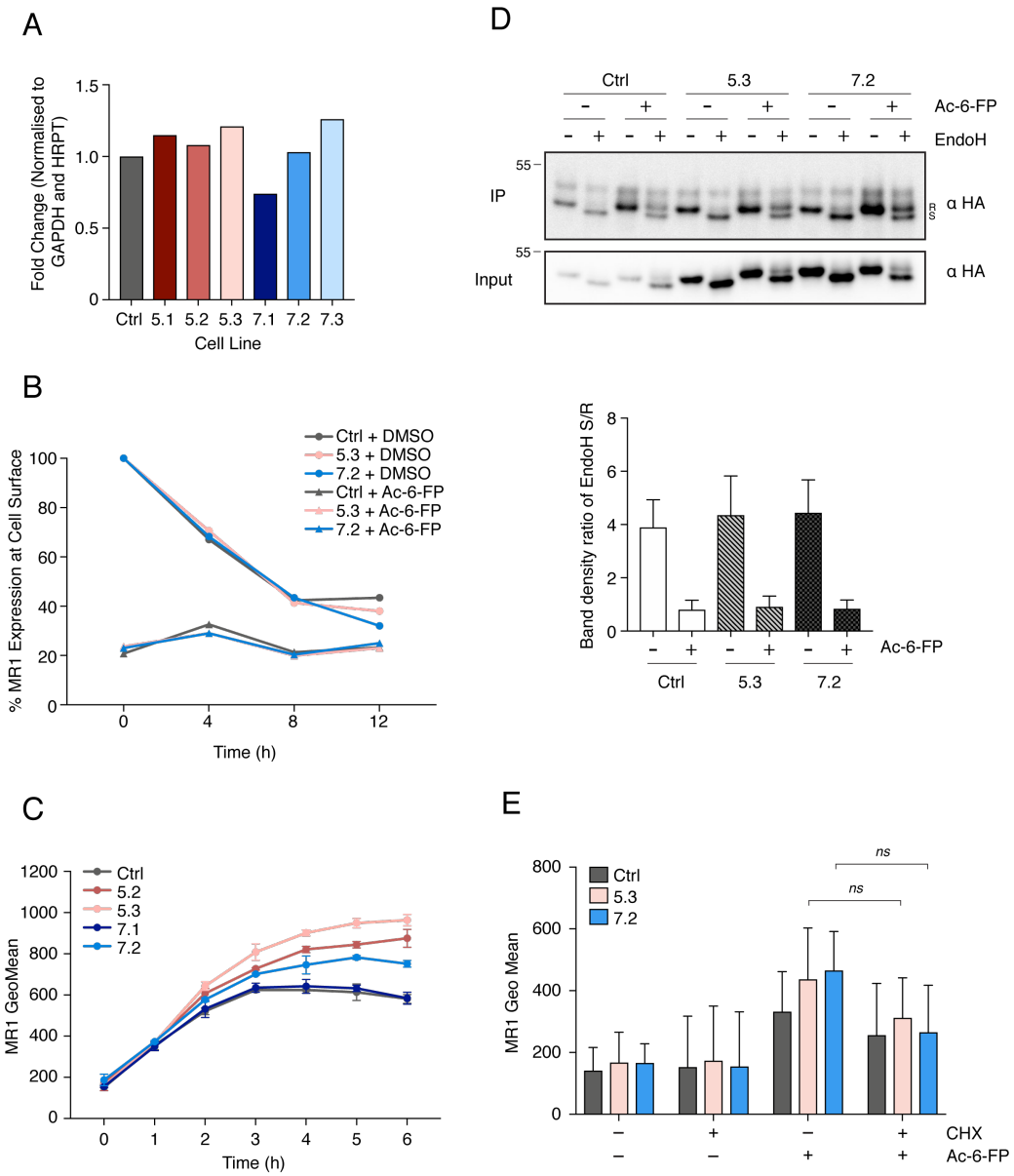
A
Fold Change (Normalised to GAPDH and HRPT)
1.5
1.0
0.5
0
Ctrl 5.1 5.2 5.3 7.1 7.2 7.3
Cell Line
B
% MR1 Expression at Cell Surface
100
80
60
40
20
0
0 4 8 12
Time (h)
Ctrl + DMSO
5.3 + DMSO
7.2 + DMSO
Ctrl + Ac-6-FP
5.3 + Ac-6-FP
7.2 + Ac-6-FP
C
MR1 GeoMean
1200
1000
800
600
400
200
0
0 1 2 3 4 5 6
Time (h)
Ctrl
5.2
5.3
7.1
7.2
D
Ctrl 5.3 7.2
Ac-6-FP
EndoH
55
IP
α HA
55
Input
α HA
Band density ratio of EndoH S/R
8
6
4
2
0
Ac-6-FP
Ctrl 5.3 7.2
E
MR1 Geo Mean
800
600
400
200
0
Ctrl
5.3
7.2
ns
ns
CHX
Ac-6-FP